


 Cite this: *RSC Adv.*, 2023, **13**, 34391

Synthesis and vectorial functionalisation of pyrazolo[3,4-c]pyridines†

 Elizabeth V. Bedwell, ^a Flavio da Silva Emery, ^b Giuliano C. Clososki^c and Patrick G. Steel ^{*a}

Heterocycles are a cornerstone of fragment-based drug discovery (FBDD) due to their prevalence in biologically active compounds. However, novel heterocyclic fragments are only valuable if they can be suitably elaborated to compliment a chosen target protein. Here we describe the synthesis of 5-halo-1*H*-pyrazolo[3,4-c]pyridine scaffolds and demonstrate how these compounds can be selectively elaborated along multiple growth-vectors. Specifically, N-1 and N-2 are accessed through protection-group and *N*-alkylation reactions; C-3 through tandem borylation and Suzuki–Miyaura cross-coupling reactions; C-5 through Pd-catalysed Buchwald–Hartwig amination; and C-7 through selective metalation with $\text{TMPPMgCl} \cdot \text{LiCl}$ followed by reaction with electrophiles or transmetalation to ZnCl_2 and Negishi cross-coupling. Linking multiple functionalisation strategies emulates a hit-to-lead pathway and demonstrates the utility of pyrazolo[3,4-c]pyridines to FBDD.

Received 1st November 2023

Accepted 9th November 2023

DOI: 10.1039/d3ra07458g

rsc.li/rsc-advances

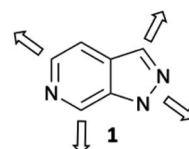
Introduction

Through the identification of weakly binding small-molecules (fragments) and their subsequent elaboration into larger more potent lead compounds, fragment-based drug discovery (FBDD) has become a major strategy for the development of new drug leads.^{1,2} Heterocyclic compounds represent attractive starting points for FBDD due to an ability to engage with the target protein through a wide variety of intermolecular interactions, coupled with the potential to optimise drug-like properties (lipophilicity, hydrogen bonding capacity, and polarity) through modification of substitution patterns. Given the requirements to compliment a protein's 3D-structure, fragment elaboration requires multiple positions, also called growth-vectors, to be decorated with different motifs to introduce new, or improve existing, binding interactions with the target. It is therefore important to be able to functionalise a given fragment along the available growth-vectors in a chemically diverse yet directionally controlled manner.

Whilst FBDD has been successfully applied to several studies, this has largely been achieved using a relatively

limited set of heteroaromatic scaffolds.³ A computational enumeration of the underutilized areas of chemical space was conducted to address this deficiency, introducing a set of novel heterocyclic motifs, the “heteroaromatic rings of the future”, as valuable inputs to inspire new drug candidates.⁴ This stimulated a number of reports describing initial access to these structures.⁵ However, further functionalisation or introduction of alternative substituent patterns often requires developing challenging *de novo* syntheses. The complexity of this synthesis limits the structural diversity of compounds that can be rapidly generated for testing and so creates a bottle-neck in FBDD programs.³ Consequently, promising fragment hits may be down-prioritised due to supposed synthetic intractability.⁶

To address these issues and increase efficiency of hit-to-lead elaboration of heterocyclic fragments, we have initiated a programme to explore late-stage functionalisation of heterocyclic cores that can be applied in a sequential and vectorially diverse manner. In this report we describe the application of complementary C–H activation methods to the vectorial elaboration of



^aDepartment of Chemistry, University of Durham, South Road, Durham, UK. E-mail: p.g.steel@durham.ac.uk

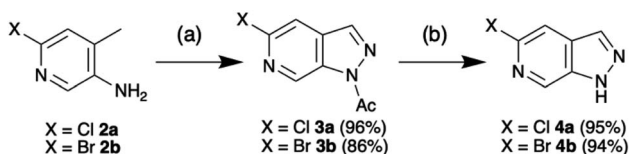
^bDepartamento de Ciências Farmacêuticas, Faculdade de Ciências Farmacêuticas de Ribeirão Preto, Universidade de São Paulo, Ribeirão Preto, SP, Brazil

^cDepartamento de Ciências Biomoleculares, Faculdade de Ciências Farmacêuticas de Ribeirão Preto, Universidade de São Paulo, Ribeirão Preto, SP, Brazil

† Electronic supplementary information (ESI) available: Optimisation of metalation chemistry, experimental procedures, analytical data and ¹H and ¹³C spectra for all compounds synthesised. See DOI: <https://doi.org/10.1039/d3ra07458g>

Fig. 1 1*H*-Pyrazolo[3,4-c]pyridine 1; the heterocyclic scaffold chosen for elaboration by vectorial functionalisation along the 4 major growth vectors.





Scheme 1 Synthesis of 5-chloro-1*H*-pyrazolo[3,4-*c*]pyridine **4a** and 5-bromo-1*H*-pyrazolo[3,4-*c*]pyridine **4b**. Conditions: (a) NaNO_2 , Ac_2O , DCE, rt – 90 °C, 20 h, (b) MeOH , NaOMe , rt, 1 h.

a 1*H*-pyrazolo[3,4-*c*]pyridine **1** scaffold (Fig. 1) as a representative example of this fragment set.

Results

Access to the 5-methoxy-pyrazolo[3,4-*c*]pyridine was recently reported by Silva Júnior *et al.* in an adaptation of the procedure first reported by Chapman and Hurst based on the classical Huisgen indazole synthesis.^{7,8} In further optimisation, introduction of dichloroethane (DCE) as a co-solvent enhanced scalability and enabled isolation of the 1-(5-halo-pyrazolo[3,4-*c*]pyridine-1-yl)ethan-1-ones **3** without need for purification (Scheme 1). Following simple deacetylation of **3** with NaOMe/MeOH , the desired 5-halo-1*H*-pyrazolo[3,4-*c*]pyridines **4** were isolated in excellent overall yield. With the scaffold in hand, the initial objective was to develop selective N-protection sequences. Using precedents based on standard indazole chemistry and tailoring reaction conditions enabled functionalisation of either N-1 or N-2.⁹

Mesylation (Ms) selectively afforded the N-1 protected product **5a** in 92% yield (Table 1, row 1). However, this group proved less useful than hoped due to the tendency for migration to C-3 as exploited by Silva Júnior *et al.*¹⁰⁻¹² Tetrahydropyran (THP) protection of the bromo-scaffold **4b** was similarly straightforward as the

N-1 isomer **6a** and N-2 isomer **6b** could be produced selectively based on reaction time (Table 1, rows 2–3) with longer reaction times favouring the thermodynamically more stable N-1 protected product.⁹ Surprisingly, the chloro-analogues **7** could not be produced selectively without significant impact on the yield. Fortunately, the N-1 and N-2 protected products, **7a** and **7b**, could be readily separated by chromatography (Table 1, row 4). Complete selectivity in the introduction of a trimethylsilyl ethoxymethyl (SEM) group was also challenging. However, by careful choice of base, either NaH or *N,N*-dicyclohexylmethylamine, predominant formation of either the N-1 or N-2 isomer could be achieved with the organic base favouring the formation of the N-2 products, **8b** and **9b** (Table 1, rows 5–8).

Finally, simple alkylation afforded the corresponding *N*-alkylated species as mixtures that could be separated by column chromatography (Table 1, rows 9–11).

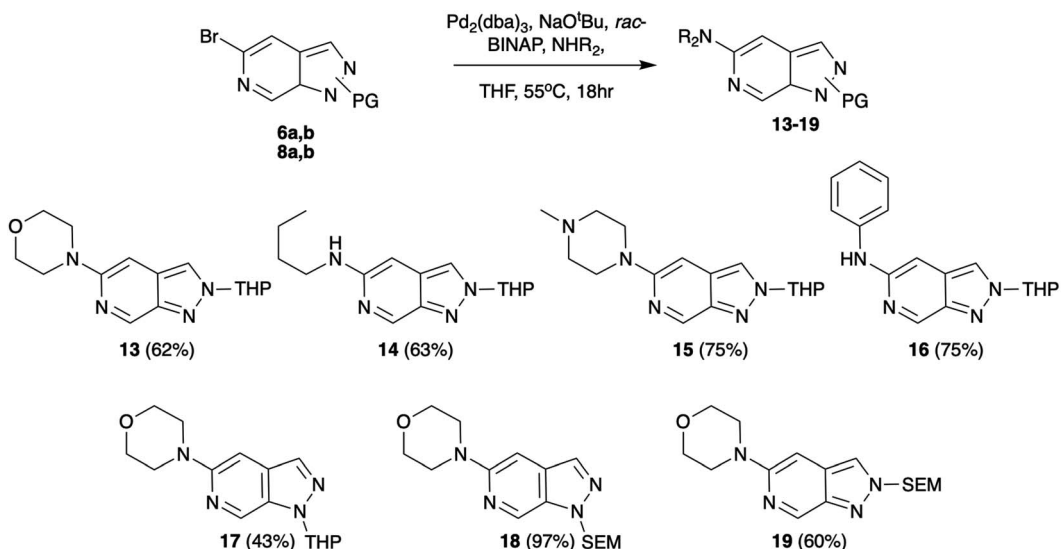
As a first vector of functionalisation, we opted to explore Buchwald–Hartwig amination at C-5 (Scheme 2). A vast array of conditions exists in the literature varying base, ligand, solvent, and reaction time depending on the substrate.¹³ Following precedents established by Slade,⁹ the combination of $\text{Pd}_2(\text{dba})_3$, *rac*-BINAP, and $\text{NaO}^\text{t}\text{Bu}$ in THF was successfully applied to reactions of **6b** with primary, secondary, and aromatic amines generating products in yields of 62–75%. These conditions were also explored for various protection group strategies which revealed the reaction of **8a** as the most successful affording **18** in 97% yield.

Selecting C-3 as the next target vector, we again took precedent from indazole chemistry in which iridium catalysed C–H borylation has been shown to occur regioselectively in this position. Consistent with the literature reports, using conditions based on those optimised by Sadler *et al.*^{14,15} both **9a** and **9b** underwent efficient borylation at the C-3 position. The utility of these boronate esters was demonstrated through *in situ* Suzuki–Miyaura cross-coupling. Whilst Suzuki–Miyaura cross-

Table 1 Selective N-1 and N-2 functionalisation of 5-halopyrazolo[3,4-*c*]pyridines

Entry	X =	Reaction conditions	R =	PG ₁ (yield)	PG ₂ (yield)
				X = Cl 7, 9, 11, 12a X = Br 6, 8, 10a	X = Cl 7, 9, 11, 12b X = Br 6, 8, 10b
1	Cl	MsCl , NaH , THF, 0 °C-rt, 2 h	-Ms	5a (92%)	5b (0%)
2	Br	DHP , $p\text{TsOH}$, DCM, rt, 2 h	-THP	6a (6%)	6b (75%)
3	Br	DHP , $p\text{TsOH}$, DCM, rt, 22 h	-THP	6a (82%)	6b (0%)
4	Cl	DHP , $p\text{TsOH}$, DCM, rt, 4 h	-THP	7a (14%)	7b (66%)
5	Br	SEMCl , Cy_2MeN , THF, 0 °C-rt, 18 h	-SEM	8a (18%)	8b (32%)
6	Br	SEMCl , NaH , THF, 0 °C-rt, 6 h	-SEM	8a (47%)	8b (26%)
7	Cl	SEMCl , NaH , THF, 0 °C-rt, 6 h	-SEM	9a (45%)	9b (29%)
8	Cl	SEMCl , Cy_2MeN , THF, 0 °C-rt, 18 h	-SEM	9a (21%)	9b (44%)
9	Br	MeI , NaH , 0 °C-rt, 1 h	-Me	10a (36%)	10b (50%)
10	Cl	MeI , NaH , 0 °C-rt, 1 h	-Me	11a (31%)	11b (42%)
11	Cl	PrI , NaH , 0 °C-rt, 24 h	-Pr	12a (27%)	12b (35%)



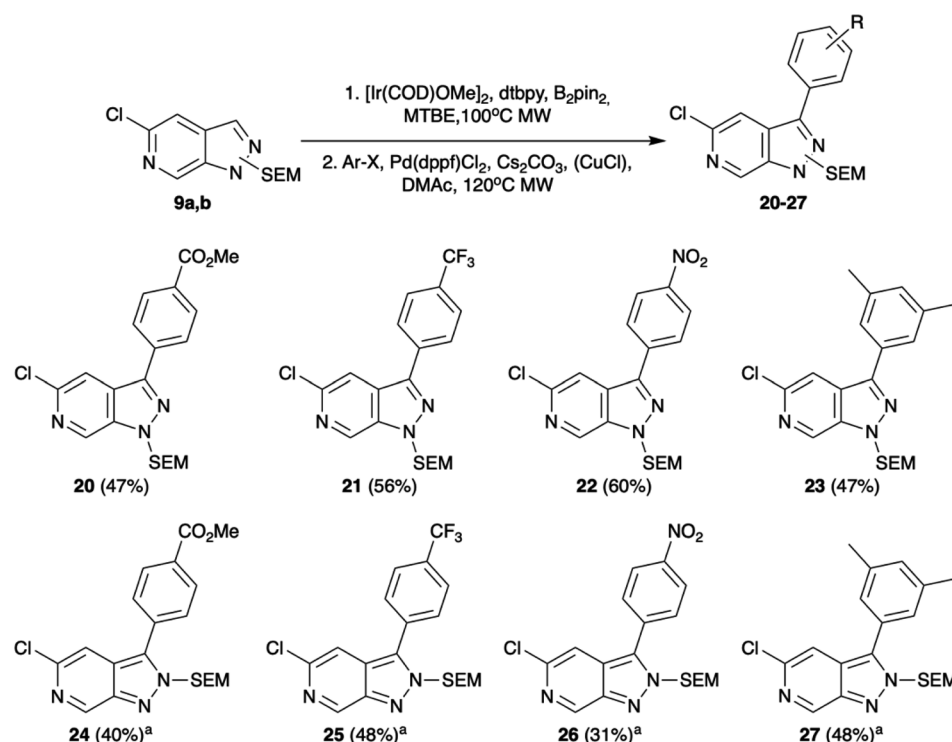


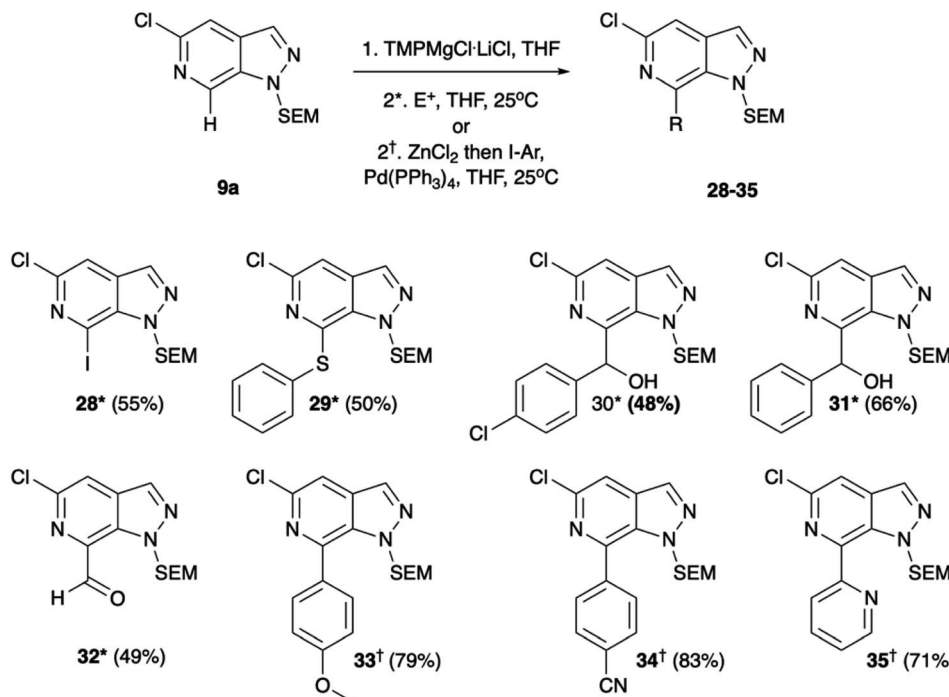
Scheme 2 Pd-catalysed Buchwald–Hartwig amination examples.

coupling of the **9a** substrate proceeded readily under standard conditions of Cs_2CO_3 and $\text{Pd}(\text{dppf})\text{Cl}_2$ in DMAc with yields of 47–60% (Scheme 3), rapid protodeborylation was a barrier to product generation for reaction of **9b**. This was addressed by use of a CuCl additive to increase the rate of transmetalation *via* formation of an intermediary Cu species.¹⁶ Under these modified conditions, the desired C-3 functionalised products could

be obtained in moderate to good overall yields (31–48%, Scheme 3).

Having established methodologies to functionalise N-1, C-3, and C-5, we then turned to the remaining vector of C-7. Initial attempts to exploit the azinyl nature of C-7 and couple the heterocycle with ⁷butyl-lithium led to nucleophilic addition at the C-7 position, albeit in very low yields. Consequently, we

Scheme 3 Tandem C–H borylation and Suzuki–Miyaura cross-coupling of **9**. Conditions: (1) $[\text{Ir}(\text{COD})\text{OMe}]_2$, dtbpy, B_2pin_2 , MTBE, $100\text{ }^\circ\text{C}$, MW, (2) Ar-X , $\text{Pd}(\text{dppf})\text{Cl}_2$, Cs_2CO_3 , DMAc, $120\text{ }^\circ\text{C}$, MW. ^aAdditional CuCl .



Scheme 4 Metalation with $\text{TMPMgCl}\cdot\text{LiCl}$ reaction with electrophiles and transmetalation with ZnCl_2 for Negishi cross-coupling. Conditions*: (1) $\text{TMPMgCl}\cdot\text{LiCl}$, THF, $-40\text{ }^\circ\text{C}$, (2) E^+ , THF, $25\text{ }^\circ\text{C}$ or conditions[†]: (1). $\text{TMPMgCl}\cdot\text{LiCl}$, THF, $-40\text{ }^\circ\text{C}$, (2) ZnCl_2 then I-Ar , $\text{Pd}(\text{PPh}_3)_4$, THF, $25\text{ }^\circ\text{C}$.

turned to more selective metalation chemistries with the mixed magnesium-lithium TMP (2,2,4,4-tetramethylpiperidine) bases.

Regioselective metalation by TMP-metal bases has been previously reported for a broad range of aromatic and heteroaromatic compounds.¹⁷⁻¹⁹ When applied to the N-1 SEM-protected analogue **9a** this afforded the desired metalation at C-7. The efficiency of the magnesiation step proved to be highly temperature dependent with optimal conversion, following trapping with iodine, being obtained at $-40\text{ }^\circ\text{C}$ (Table S1, ESI[†]). To demonstrate the broad scope of this chemistry, the intermediate organomagnesium species were treated with a variety of electrophiles including aldehydes, diphenyl disulfide, and DMF for yields of 48–66%. Alternatively, transmetalation with ZnCl_2 afforded a range of arylated products via Negishi cross-coupling chemistry with yields of 71–83% (Scheme 4). Interestingly, $\text{TMPMgCl}\cdot\text{LiCl}$ treatment of the N-2 SEM-protected compound **13b** led to metalation at C-3 instead of C-7 (Scheme 5). However, this reaction was inefficient and produced a complex mixture of products.

As the C-3 vector had already been thoroughly explored through Ir-catalysed borylation, this route was not pursued further.

While individual elaboration along each growth vector is a valuable tool to explore fragment space, it is likely that an FBDD optimisation may require multiple vectors of growth. As a final aspect we, therefore, sought to demonstrate how these functionalisation strategies could be combined to emulate a hit-to-lead pathway common to medicinal chemistry development.

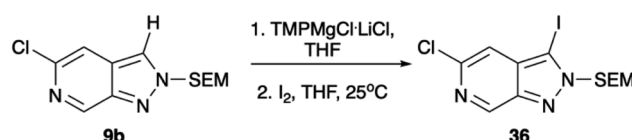
In the first sequence, a combination of C-3 borylation, Suzuki-Miyaura cross-coupling and a tandem N-methylation/SEM-deprotection was explored (Scheme 6A). In the case of N-

2 SEM-protected compound **25**, reaction with $[\text{Me}_3\text{O}][\text{BF}_4]$ (trimethyloxonium tetrafluoroborate) saw efficient formation of the N1-methylated product **37**. In the case of the N-1 SEM-protected isomers, methylation of N-2 occurred readily with $[\text{Me}_3\text{O}][\text{BF}_4]$ to afford the methyl salts **38** and **39**.

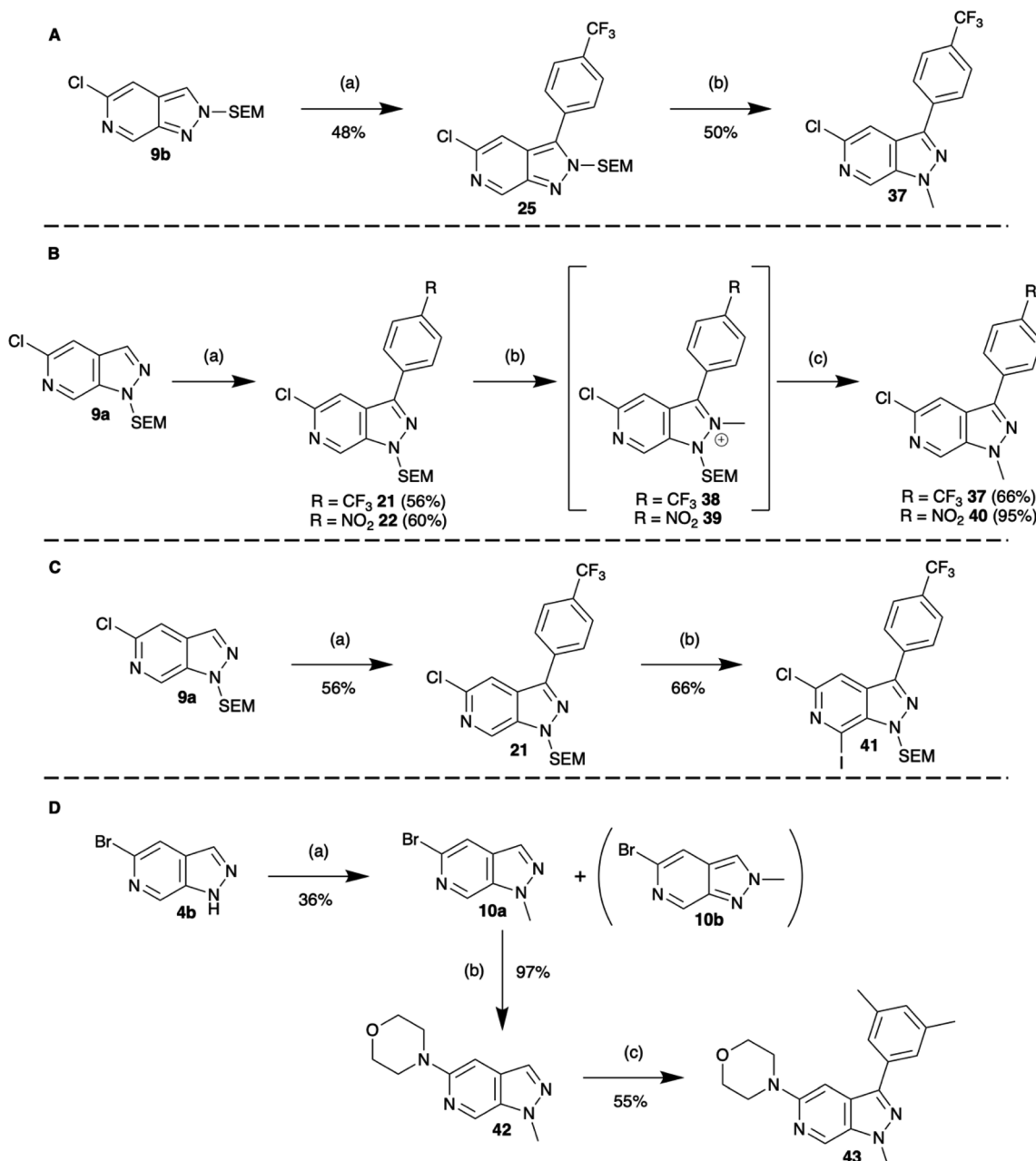
However, surprisingly, acid catalysed SEM-deprotection with TFA did not give the expected conversion to N2-methylated compounds, instead, ipso methylation at N-1 was observed and **37** and **40** were isolated (Scheme 6B). It is likely that these observations reflect the greater thermodynamic stability of the 1*H*-pyrazolo[3,4-*c*]pyridine core.

A second two stage sequence paired C-3 borylation Suzuki-Miyaura cross-coupling functionalisation with C-7 $\text{TMPMgCl}\cdot\text{LiCl}$ metalation and electrophilic trapping with iodine to give **41** (Scheme 6C).

Finally, extensions to more elaborate three-vector functionalisation sequences are also possible. Exemplified in Scheme 6D showing a three-step sequence from fragment **4b** to compound **43**. Importantly, despite the increasing



Scheme 5 Metalation with $\text{TMPMgCl}\cdot\text{LiCl}$ reaction with iodine. Conditions: (1) $\text{TMPMgCl}\cdot\text{LiCl}$, THF, $-78\text{ }^\circ\text{C}$, 30 min, (2) I_2 , THF, $25\text{ }^\circ\text{C}$, 1 h.



Scheme 6 Multiple-vector elaboration sequences. (A) C-3 borylation, Suzuki–Miyaura cross-coupling with a tandem *N*-methylation/SEM-deprotection, conditions: (a) (1) [Ir(COD)OMe]₂, dtbpy, B₂pin₂, MTBE, 100 °C MW, 2. C₇H₄F₃Br, Pd(dppf)Cl₂, Cs₂CO₃, CuCl, DMAc, 120 °C MW, (b) [Me₃O][BF₄]₁, EtOAc, rt, 18 h. (B) C-3 borylation, Suzuki–Miyaura cross-coupling with a tandem *N*-methylation/SEM-deprotection, conditions: (a) (1) [Ir(COD)OMe]₂, dtbpy, B₂pin₂, MTBE, 100 °C MW, 2. ArX, Pd(dppf)Cl₂, Cs₂CO₃, DMAc, 120 °C MW, (b) [Me₃O][BF₄]₁, EtOAc, rt, 6 h, (c) TFA, DCM, rt, 20 h. (C) C-3 borylation, Suzuki–Miyaura cross-coupling with C-7 TMPMgCl/LiCl metatlation and electrophilic trapping with iodine, conditions: (a) (1) [Ir(COD)OMe]₂, dtbpy, B₂pin₂, MTBE, 100 °C MW, (2) C₇H₄F₃Br, Pd(dppf)Cl₂, Cs₂CO₃, DMAc, 120 °C MW, (b) (1) TMPMgCl/LiCl, THF, –40 °C, 30 min (2) I₂, THF, rt, 1 h. (D) *N*-Methylation, Buchwald–Hartwig amination, and C-3 borylation, Suzuki–Miyaura cross-coupling, conditions: (a) MeI, NaH, THF, rt, 45 min, (b) Pd₂(dba)₃, NHR₂, NaO^tBu, *rac*-BINAP, THF, 55 °C, 18 h, (c) (1) [Ir(COD)OMe]₂, dtbpy, B₂pin₂, MTBE, 100 °C MW 30 min (2) C₈H₉I, Pd(dppf)Cl₂, Cs₂CO₃, DMAc, 120 °C MW 2 h.

complexity, in each of these processes the yield of each step was comparable to that obtained earlier. Other sequences of elaboration can be endlessly imagined combining the chemistry explored herein to realise an expansive library of heterocyclic compounds.

Conclusion

In summary, we have developed efficient synthetic routes to 5-halo-1*H*-pyrazolo[3,4-*c*]pyridine scaffolds and demonstrated how these compounds can be selectively elaborated along multiple reaction vectors. The pyrazolo[3,4-*c*]pyridine core

has begun to attract attention as a therapeutic agent due to its structural similarity to purine.^{20–23} Purine derivatives have a broad range of applications, as anti-inflammatory, anti-viral, and anti-cancer agents, arising from the prevalence of purine-based biological compounds and, subsequently, the variety of cellular proteins that contain purine-binding pockets.²⁰ Whilst routes have been reported for related products with different substituent patterns around the pyrazolo[3,4-*c*]pyridine core, most of these require discrete synthetic endeavour.^{23–25} The chemistry described here allows introduction of functionality at C-3, C-5 and C-7 and as such is complimentary to the recent related report by Silva Júnior *et al.* which describes alternative C-4 functionalisation of a 5-methoxy analogue.¹⁰

Importantly, through careful control of reaction sequence it is possible to selectively explore growth in a combination of vectors with no loss in synthetic efficiency.

Overall, the late-stage functionalisation sequences described here provide practical advantages, particularly for the introduction of structural diversity required for fragment-elaboration in an FBDD hit-to-lead evolution pipeline. Extensions of these ideas to other heterocyclic cores are in progress and the results of this will be reported in due course.

Experimental section

All solvents and reagents were purchased from commercial suppliers and used without further purification unless otherwise stated below. Final compound purification by flash column chromatography was performed on a CombiFlash® System from Teledyne Isco equipped with an UV-light detector using prepacked silica RediSep Rf cartridges with the stated solvent gradient. Crude mixtures to be purified were dry loaded onto silica (normal phase) or Celite® 545 (reverse phase) prior to running the column. NMR spectra were recorded on the following instruments: Bruker Neo 700 MHz spectrometer with operating frequencies of 700 MHz for ¹H and 175 MHz for ¹³C; Varian VNMRS-600 with operating frequencies of 600 MHz for ¹H and 150 MHz for ¹³C NMR; and Varian VNMRS-400 with operating frequencies of 400 MHz for ¹H and 376 MHz for ¹⁹F NMR. Spectra were referenced relative to CDCl₃ (δ _H 7.26 ppm, δ _C 77.16 ppm), CD₃OD (δ _H 4.87 ppm, δ _C 49.00 ppm), or DMSO (δ _H 2.50 ppm, δ _C 39.52 ppm). Chemical shifts are reported in parts per million (ppm), coupling constants (*J*) in hertz (Hz) and multiplicity as singlet (s), doublet (d), triplet (t), quartet (q), pentet (p), sextet (s), multiplet (m) or a combination thereof. All *J* values are *J*_{H–H} unless otherwise stated. All ¹H NMR and ¹³C NMR spectral assignments were made with the aid of ¹H–¹H COSY, ¹H–¹H NOESY, ¹H–¹³C HSQC and ¹H–¹³C HMBC NMR experiments. Infra-red spectra were recorded on a PerkinElmer Paragon 1000 FT-IR spectrometer or a PerkinElmer RX FT-IR spectrometer with Golden Gate Diamond ATR apparatus. IR assignments are reported in wavenumbers (cm^{−1}).

Melting points were recorded on Thermo Scientific Electrothermal IA9100 Digital Melting Point apparatus. Thin layer chromatography was performed using Merck F254 silica gel

60 aluminium sheets pre-coated with silica gel. High resolution mass spectrometry (HRMS) and liquid chromatography–mass spectrometry (LC-MS) were recorded on a Waters TQD mass spectrometer ESI-LC water (0.1% formic acid): MeCN/MeOH, flow rate 0.6 mL min^{−1} with a UPLC BEH C18 1.7 μ m (2.1 mm × 50 mm) column. Gas chromatography mass spectrometry (GCMS) was carried out on a Shimadzu QP2010-Ultra with a temperature gradient 50–300 °C and a hold time of 5 min, using a Rxi-17Sil MS (0.15 μ m × 10 m × 0.15 mm) column.

Substrate synthesis

1'-{5-Chloro-1*H*-pyrazolo[3,4-*c*]pyridin-1-yl}ethan-1'-one 3a. Ac₂O (33 mL, 0.35 mol, 10.0 eq.) was added to a solution of 6-chloro-4-methylpyridin-3-amine **2a** (5.00 g, 35 mmol, 1.00 eq.) in DCE (140 mL) and stirred at room temperature for 90 minutes under nitrogen. NaNO₂ (9.68 g, 0.14 mol, 4.00 eq.) was added and the reaction mixture stirred at room temperature for 3 hours, then heated overnight at 90 °C. The reaction mixture was concentrated under reduced pressure then diluted with NaHCO₃ (150 mL). The product was extracted into EtOAc (5 × 100 mL) then washed with H₂O (4 × 100 mL) and brine (2 × 100 mL), dried over MgSO₄, filtered, and concentrated under reduced pressure to give 1'-{5-chloro-1*H*-pyrazolo[3,4-*c*]pyridin-1-yl}ethan-1'-one **3a** as a white solid (6.57 g, 34 mmol, 96%) with mp 138–139 °C. δ _H (400 MHz, chloroform-*d*) 9.56 (1*H*, s, 7-*H*), 8.15 (1*H*, s, 3-*H*), 7.69 (1*H*, s, 4-*H*), 2.81 (3*H*, s, C(O)CH₃); δ _C (101 MHz, chloroform-*d*) 170.3 (C=O), 144.7 (C-5), 138.0 (C-7), 137.8 (C-3), 134.7 (C-7a), 133.8 (C-3a), 114.8 (C-4), 22.6 (C(O)CH₃); *V*_{max} (ATR) 1729 (C=O), 1390, 1353, 634 cm^{−1}; LC-MS (ES+) [M (35Cl) + H] 196.069, [M (37Cl) + H] 198.007, [M (35Cl) + H – COCH₃] 154.035, [M (37Cl) + H – COCH₃] 156.011; HRMS (ES+) found [M + H]⁺ 196.0290, C₈H₇N₃O³⁵Cl requires *M* 196.0278. The analytical data were consistent with the literature.⁷

5-Chloro-1*H*-pyrazolo[3,4-*c*]pyridine 4a. NaOMe (0.150 g, 2.8 mmol, 0.25 eq.) was added to a solution of 1'-{5-chloro-1*H*-pyrazolo[3,4-*c*]pyridin-1-yl}ethan-1'-one **3a** (2.0 g, 10 mmol, 1.00 eq.) in anhydrous MeOH (50 mL) and stirred at room temperature for 15 minutes. The reaction was quenched by addition of HCl : MeOH 1 : 100 (8 mL) until acidic pH and concentrated under reduced pressure. The crude product was taken up in H₂O (75 mL) then adjusted to pH 10 by addition of aqueous NaOH then extracted with EtOAc (3 × 100 mL). The combined organic layers were washed with brine (75 mL), dried over MgSO₄, filtered and concentrated to afford 5-chloro-1*H*-pyrazolo[3,4-*c*]pyridine **4a** as a white solid (1.5 g, 10 mmol, 95%) with mp 225–226 °C. δ _H (400 MHz, methanol-*d*₄) 8.80 (1*H*, s, 7-*H*), 8.15 (1*H*, d, *J* = 1.2 Hz, 3-*H*), 7.82 (1*H*, d, *J* = 1.2 Hz, 4-*H*); δ _C (101 MHz, methanol-*d*₄) 141.0 (C-5), 137.6 (C-7a), 135.1 (C-7), 134.2 (C-3), 131.2 (C-3a), 115.6 (C-4); *V*_{max} (ATR) 909, 736, 652 cm^{−1}; LC-MS (ES+) [M (35Cl) + H] 154.113, [M (37Cl) + H] 156.128; HRMS (ES+) found [M + H]⁺ 154.0167, C₆H₅N₃³⁵Cl requires *M* 154.0172.

General procedure A – for Buchwald–Hartwig amination. Pd₂dba₃ (0.05 eq.), *rac*-BINAP (0.12 eq.), NaO^tBu (3.00 eq.), and the stated protected pyrazolo[3,4-*c*]pyridine (1.00 eq.) were sealed under a nitrogen atmosphere. The stated amine (1.10

eq.) was added under nitrogen, followed by dry THF (0.1 M). The deep red solution was stirred overnight at 55 °C until LCMS analysis confirmed complete conversion of the starting substrate. The reaction was cooled to room temperature, diluted with EtOAc and filtered through Celite, washing the cake with additional EtOAc. This solution was concentrated under reduced pressure. The product was purified by silica gel flash column chromatography using the stated solvent system.

4-[2'-(Oxan-2'-yl)-2H-pyrazolo[3,4-c]pyridin-5'-yl]morpholine

13. General procedure A was applied to 5-bromo-2-(oxan-2'-yl)-2H-pyrazolo[3,4-c]pyridine **6b** (0.080 g, 0.28 mmol, 1.00 eq.) with morpholine (0.03 mL, 0.31 mmol, 1.10 eq.). After purification by silica gel flash column chromatography (EtOAc:Pet ether 40–60 0–100%), 4-[2'-(oxan-2'-yl)-2H-pyrazolo[3,4-c]pyridin-5'-yl]morpholine **13** was isolated as a dark green oil (0.051 g, 0.18 mmol, 62%). δ_{H} (600 MHz, chloroform-*d*) 9.05 (1H, t, *J* = 1.2 Hz, 7'-*H*), 7.99 (1H, d, *J* = 1.2 Hz, 3'-*H*), 6.58 (1H, d, *J* = 1.2 Hz, 4'-*H*), 5.66 (1H, dd, *J* = 8.2, 4.1 Hz, 2'-*H*), 4.13–4.07 (1H, m, 6"-*H*), 3.91–3.87 (4H, m, 2,6"-*H*), 3.77 (1H, ddd, *J* = 11.7, 10.4, 3.0 Hz, 6"-*H*), 3.40–3.35 (4H, m, 3,5-H), 2.20 (2H, ddd, *J* = 10.0, 8.2, 4.1 Hz, 3"-*H*), 2.07–2.01 (1H, m, 4"-*H*), 1.79–1.63 (1H, m, 4"-*H*), 1.79–1.63 (2H, m, 5"-*H*); δ_{C} (151 MHz, chloroform-*d*) 154.1 (C-5'), 143.3 (C-7'), 142.7 (C-7'a), 126.1 (C-3'a), 119.3 (C-3'), 91.8 (C-4), 89.2 (C-2'), 67.8 (C-6'), 66.9 (C-2,6), 48.1 (C-3,5), 31.2 (C-3"), 24.9 (C-5"), 21.9 (C-4"); V_{max} (ATR) 1495, 1200, 0998, 729 cm^{-1} ; LC-MS (ES+) [M + H]⁺ 289.294; HRMS (ES+) found [M + H]⁺ 289.1670, C₁₅H₂₁N₄O₂ requires M 298.1665.

General procedure B – for tandem borylation and Suzuki-Miyaura cross-coupling

[Ir(COD)OMe]₂ (0.025 eq.), B₂pin₂ (1.10 eq.), and dtbpy (0.05 eq.) were sealed in an oven-dried microwave reaction vial and degassed with N₂/vacuum cycling. A solution of the SEM-protected pyrazolo[3,4-c]pyridine in anhydrous MTBE (0.4 M) was added under nitrogen. The reaction mixture was heated in a microwave reactor at 100 °C until GCMS analysis showed complete borylation had occurred, then concentrated under reduced pressure to afford the crude boronate ester. To the crude boronate ester was added Cs₂CO₃ (1.00 eq.), Pd(OAc)₂ (0.025 eq.), 1,1'-bis(diphenylphosphino)ferrocene (dpfpf) (0.050 eq.), CuCl (1.00 eq.), the aryl halide (1.10 eq.) and anhydrous DMAc (1 M) under nitrogen. The reaction mixture was heated in a microwave reactor at 120 °C until GCMS analysis showed no boronate ester remained. The reaction mixture was filtered through Celite® and the residue washed with EtOAc. The combined filtrates were concentrated under reduced pressure, and the residue was dissolved in H₂O then extracted with EtOAc. The combined organic layers were washed with brine, dried over MgSO₄, filtered, and concentrated. The product was purified by silica gel flash column chromatography using the stated solvent system.

5-Chloro-3-(4'-nitrophenyl)-1-[2'-(trimethylsilyl)ethoxy]methyl-1H-pyrazolo[3,4-c]pyridine **22.**

General procedure B was applied to 5-chloro-1-[2'-(trimethylsilyl)ethoxy]methyl-1H-pyrazolo[3,4-c]pyridine **9a** (0.150 g, 0.53 mmol, 1.00 eq.) with 1-iodo-4-nitrobenzene (0.145 g, 0.58 mmol, 1.10 eq.). After purification by silica gel flash column chromatography (EtOAc:hexanes 0–20%), 5-chloro-3-(4'-nitrophenyl)-1-[2'-(trimethylsilyl)ethoxy]methyl-1H-pyrazolo[3,4-c]pyridine **22** was isolated as a white solid (0.129 g, 0.32 mmol, 60%) with mp

111–113 °C. δ_{H} (600 MHz, chloroform-*d*) 8.96 (1H, d, *J* = 1.2 Hz, 7-H), 8.41–8.35 (2H, m, 3',5'-H), 8.15–8.09 (2H, m, 2',6'-H), 7.94 (1H, d, *J* = 1.2 Hz, 4-H), 5.86 (2H, s, NCH₂O), 3.64–3.59 (2H, m, OCH₂CH₂), 0.95–0.88 (2H, m, CH₂CH₂SiMe₃), −0.06 (9H, s, SiCH₃); δ_{C} (151 MHz, Chloroform-*d*) 147.7 (C-4'), 143.0 (C-5), 141.4 (C-3), 138.1 (C-1'), 137.1 (C-7a), 134.4 (C-7), 129.2 (C-3a), 127.6 (C-3', 5'), 124.4 (C-2', 6'), 114.3 (C-4), 79.1 (NCH₂O), 67.4 (OCH₂CH₂), 17.7 (CH₂CH₂Si), −1.5 (Si(CH₃)₃); V_{max} (ATR) 1516 (N=O asymmetric), 1349 (N=O symmetric), 1074, 857, 834, 821 cm^{-1} ; LC-MS (ES+) [M (³⁵Cl) + H]⁺ 405.282 [M (³⁷Cl) + H]⁺ 407.297; HRMS (ES+) found [M + H]⁺ 405.1153, C₁₈H₂₂N₄O₃·Si³⁵Cl requires M 405.1150.

General procedure C – for tandem borylation and Suzuki-Miyaura cross-coupling with CuCl

[Ir(COD)OMe]₂ (0.025 eq.), B₂pin₂ (1.10 eq.), and dtbpy (0.05 eq.) were sealed in an oven-dried microwave reaction vial and degassed with N₂/vacuum cycling. A solution of the SEM-protected pyrazolo[3,4-c]pyridine in anhydrous MTBE (0.4 M) was added under nitrogen. The reaction mixture was heated in a microwave reactor at 100 °C until GCMS analysis showed complete borylation had occurred, then concentrated under reduced pressure to afford the crude boronate ester. To the crude boronate ester was added Cs₂CO₃ (1.00 eq.), Pd(OAc)₂ (0.025 eq.), 1,1'-bis(diphenylphosphino)ferrocene (dpfpf) (0.050 eq.), CuCl (1.00 eq.), the aryl halide (1.10 eq.) and anhydrous DMAc (1 M) under nitrogen. The reaction mixture was heated in a microwave reactor at 120 °C until GCMS analysis showed no boronate ester remained. The reaction mixture was filtered through Celite® and the residue washed with EtOAc. The combined filtrates were concentrated under reduced pressure, and the residue was dissolved in H₂O then extracted with EtOAc. The combined organic layers were washed with brine, dried over MgSO₄, filtered, and concentrated. The product was purified by silica gel flash column chromatography using the stated solvent system.

5-Chloro-3-(3',5'-dimethylphenyl)-2-[2'-(trimethylsilyl)ethoxy]methyl-2H-pyrazolo[3,4-c]pyridine **27.** General procedure C was applied to 5-chloro-2-[2'-(trimethylsilyl)ethoxy]methyl-2H-pyrazolo[3,4-c]pyridine **9b** (0.100 g, 0.35 mmol, 1.00 eq.) with 1-iodo-3,5-dimethylbenzene (0.06 mL, 0.39 mmol, 1.10 eq.). Purification by silica gel flash column chromatography (EtOAc:Pet ether 40–60 0–20%) afforded 5-chloro-3-(3',5'-dimethylphenyl)-2-[2'-(trimethylsilyl)ethoxy]methyl-2H-pyrazolo[3,4-c]pyridine **27** as a yellow oil (0.065 g, 0.17 mmol, 48%). δ_{H} (600 MHz, chloroform-*d*) 9.11 (1H, d, *J* = 1.2 Hz, 7-H), 7.57 (1H, d, *J* = 1.2 Hz, 4-H), 7.30–7.27 (2H, m, 2',6'-H), 7.17–7.14 (1H, m, 4'-H), 5.72 (2H, s, NCH₂O), 3.86–3.80 (2H, m, OCH₂CH₂), 2.43 (6H, q, *J* = 0.7 Hz, Ar-CH₃), 0.98–0.93 (2H, m, CH₂CH₂Si), −0.01 (9H, s, Si(CH₃)₃); δ_{C} (151 MHz, chloroform-*d*) 144.6 (C-7), 143.9 (C-5), 140.6 (C-7'a), 139.0 (C-3',5'), 137.2 (C-3), 131.3 (C-4'), 127.8 (C-1'), 127.3 (C-2',6'), 125.4 (C-3a), 113.5 (C-4), 79.8 (NCH₂O), 68.1 (OCH₂CH₂), 21.4 (Ar-CH₃), 17.9 (CH₂CH₂Si), −1.4 (Si(CH₃)₃); V_{max} (ATR) 1465, 1106, 1085, 1061, 858, 838 cm^{-1} ; LC-MS (ES+) [M (³⁵Cl) + H]⁺ 388.333 [M (³⁷Cl) + H]⁺ 390.347; HRMS



(ES⁺) found [M + H]⁺ 388.1598, C₂₀H₂₇³⁵ClN₃OSi requires M 388.1612.

General procedure D – for deproto-metalation by TMPMgCl⁺LiCl and trapping with an electrophile

An oven dried RBF was charged with a solution of the stated substrate (1.00 eq.) in dry THF (0.5 M) and cooled to -40 °C under a nitrogen atmosphere. TMPMgCl⁺LiCl in THF (2.00 eq.) was added dropwise and the reaction was stirred for 30 min at -40 °C. The corresponding electrophile was added at -40 °C, then the reaction was stirred at room temperature for the time stated. The reaction was quenched with NaHSO₃ sat. solution and the crude product extracted with EtOAc, then the combined organic layers were washed with brine, dried over MgSO₄, filtered, and concentrated under reduced pressure. The product was purified by silica gel flash column chromatography using the stated solvent system.

5-Chloro-7-(phenylsulfanyl)-1-[(2'-trimethylsilyl)ethoxy]methyl-1*H*-pyrazolo[3,4-*c*]pyridine 29. General procedure D was applied to 5-chloro-1-[(2'-trimethylsilyl)ethoxy]methyl-1*H*-pyrazolo[3,4-*c*]pyridine 9a (0.150 g, 0.53 mmol, 1.00 eq.) with electrophile S₂Ph₂ (0.173 g, 0.79 mmol, 1.50 eq.) for 18 hours. Purification by reverse phase column chromatography (MeCN:H₂O 0–100%) afforded 5-chloro-7-(phenylsulfanyl)-1-[(2'-trimethylsilyl)ethoxy]methyl-1*H*-pyrazolo[3,4-*c*]pyridine 29 as a yellow oil (0.104 g, 0.27 mmol, 50%). δ_{H} (700 MHz, chloroform-*d*) 7.98 (1H, s, 3-*H*), 7.58 (2H, dd, *J* = 7.5, 2.1 Hz, 2'', 6'', 7-*H*), 7.43 – 7.40 (2H, m, 3'', 5'', 7-*H*), 7.43–7.40 (1H, m, 4'', 7-*H*), 7.39 (1H, s, 4-*H*), 6.09 (2H, s, NCH₂O), 3.64–3.59 (2H, m, OCH₂CH₂), 0.95–0.90 (2H, m, OCH₂CH₂Si), -0.04 (9H, s, Si(CH₃)₃); δ_{C} (176 MHz, chloroform-*d*) 143.1 (C-7), 140.9 (C-5), 134.4 (C-2'', 6''), 134.3 (C-7a), 133.1 (C-3), 132.3 (C-3a), 129.4 (C-1''), 129.3 (C-3'', 5''), 129.1 (C-4''), 111.6 (C-4), 79.9 (NCH₂O), 66.7 (OCH₂CH₂Si), 17.9 (OCH₂CH₂Si), -1.3 (Si(CH₃)₃); V_{max} (ATR) 1078, 856, 833, 796, 689 cm⁻¹; LC-MS (ES+) [M (sup35Cl) + H] 392.209 [M (sup37Cl) + H] 394.223; HRMS found [M + H]⁺ 392.1020, C₁₈H₂₃³⁵ClN₃OSi requires M 392.1020.

General procedure E – for deproto-metalation by TMPMgCl⁺LiCl and transmetalation to Zn for Negishi cross-coupling

An oven-dried reaction vessel was charged with a solution of the substrate (1.00 eq.) in dry THF (0.5 M), the atmosphere was exchange to nitrogen, and the solution cooled to -40 °C. TMPMgCl⁺LiCl in THF (2.00 eq.) was added dropwise and the reaction was stirred for 30 minutes at -40 °C. A solution of ZnCl₂ (1.00 eq.) in THF (1 M) was added and the reaction stirred for 30 minutes at -40 °C. In a separate oven-dried reaction vessel, a solution of the corresponding (hetero)aryl halide (1.50 eq.) and Pd(PPh₃)₄ (0.05 eq.) in THF (0.5 M) were stirred at room temperature for 30 minutes. This solution was added to the main reaction mixture at -40 °C, then the reaction was stirred at room temperature overnight. The reaction was quenched with NH₄Cl sat. solution and the crude product extracted with EtOAc, then the combined organic layers were washed with brine, dried over MgSO₄, filtered, and concentrated under

reduced pressure. The product was purified by silica gel flash column chromatography using the stated solvent system.

4-(5'-Chloro-1'-(2''-(trimethylsilyl)ethoxy)methyl-1*H*-pyrazolo[3,4-*c*]pyridin-7'-yl)benzonitrile 34. General procedure E was applied to 5-chloro-1-[(2'-trimethylsilyl)ethoxy]methyl-1*H*-pyrazolo[3,4-*c*]pyridine 9a (0.100 g, 0.35 mmol, 1.00 eq.) with 4-iodobenzonitrile (0.121 g, 0.55 mmol, 1.50 eq.). Purification by reverse phase column chromatography (MeCN:H₂O 50–100%) afforded 4-(5'-chloro-1'-(2''-(trimethylsilyl)ethoxy)methyl-1*H*-pyrazolo[3,4-*c*]pyridin-7'-yl)benzonitrile 34 as a cream solid (0.113 g, 0.29 mmol, 83%) with mp 90–94 °C.

δ_{H} (600 MHz, CDCl₃) 8.13 (1H, s, 3'-*H*), 7.85 (2H, d, *J* = 7.9 Hz, 2,6-*H*), 7.81 (2H, d, *J* = 7.9 Hz, 3,5-*H*), 7.71 (1H, s, 4'-*H*), 5.38 (2H, s, NCH₂O), 3.40 (2H, m, OCH₂CH₂), 0.77 (2H, m, OCH₂CH₂Si), -0.07 (9H, s, Si(CH₃)₃); δ_{C} (151 MHz, CDCl₃) 143.0 (C-7'), 141.4 (C-4), 140.9 (C-5'), 133.7 (C-3'a), 133.6 (C-7'a), 133.4 (C-3'), 132.1 (C-2,6), 130.2 (C-3,5), 118.3 (C≡N), 114.3 (C-4'), 113.4 (C-1), 78.4 (NCH₂O), 66.8 (OCH₂CH₂), 17.7 (OCH₂CH₂Si), -1.5 (Si(CH₃)₃); V_{max} (ATR) 2230 (C≡N), 1070, 856, 837, 815 cm⁻¹; LC-MS (ES+) [M (sup35Cl) + H] 385.330 [M (sup37Cl) + H] 387.307; HRMS found [M + H]⁺ 385.1250, C₁₉H₂₂³⁵ClN₄OSi requires M 385.1251.

Author contributions

EVB designed and conducted experiments; EVB and PGS drafted the manuscripts; FE, GCC and PGS conceived the project, designed experiments, and supervised the work; PGS secured the funding. All authors reviewed and edited the manuscript and approved the final submitted version.

Conflicts of interest

There are no conflicts to declare.

Acknowledgements

We thank EPSRC (studentship to EVB EP/T518001/1) the GCRF and Newton Fund Consolidation Account (EP/X527713/1) and Fundação de Amparo à Pesquisa do Estado de São Paulo (FAPESP) - (Grant to GCC 22/05327-7) for financial support of this work; Dr Juan Aguilar(DU), Peter Stokes (DU), and Dr Aileen Congreve (DU) for assistance with compound characterisation data; and Victor Hugo (USP-RP) for guidance with metalation chemistry.

References

- 1 P. Kirsch, A. M. Hartman, A. K. H. Hirsch and M. Empting, *Mol.*, 2019, **24**, 4309.
- 2 L. Walsh, D. A. Erlanson, I. J. P. de Esch, W. Jahnke, A. Woodhead and E. Wren, *J. Med. Chem.*, 2023, **66**, 1137–1156.
- 3 R. D. Taylor, M. MacCoss and A. D. Lawson, *J. Med. Chem.*, 2014, **57**, 5845–5859.
- 4 W. R. Pitt, D. M. Parry, B. G. Perry and C. R. Groom, *J. Med. Chem.*, 2009, **52**, 2952–2963.



5 K. Passador, S. Thorimbert and C. Botuha, *Synth.*, 2019, **51**, 384–398.

6 G. Chessari, R. Grainger, R. S. Holvey, R. F. Ludlow, P. N. Mortenson and D. C. Rees, *Chem. Sci.*, 2021, **12**, 11976–11985.

7 D. Chapman and J. Hurst, *J. Chem. Soc., Perkin Trans. 1*, 1980, 2398–2404.

8 P. E. da Silva Júnior, L. C. D. Rezende, J. P. Gimenes, V. G. Maltarollo, J. Dale, G. H. G. Trossini, F. da Silva Emery and A. Ganesan, *RSC Adv.*, 2016, **6**, 22777–22780.

9 D. J. Slade, N. F. Pelz, W. Bodnar, J. W. Lampe and P. S. Watson, *J. Org. Chem.*, 2009, **74**, 6331–6334.

10 P. E. da Silva Júnior, S. M. G. de Melo, M. H. de Paula, R. Vesseccchi, T. Opatz, J. E. H. Day, A. Ganesan and F. da Silva Emery, *Org. Biomol. Chem.*, 2022, **20**, 7483–7490.

11 B. Prasad, R. Adepu, S. Sandra, D. Rambabu, G. R. Krishna, C. M. Reddy, G. S. Deora, P. Misra and M. Pal, *Chem. Commun.*, 2012, **48**, 10434–10436.

12 S. Searles and S. Nukina, *Chem. Rev.*, 1959, **59**, 1077–1103.

13 R. Dorel, C. P. Grugel and A. M. Haydl, *Angew. Chem., Int. Ed.*, 2019, **58**, 17118–17129.

14 S. A. Sadler, A. C. Hones, B. Roberts, D. Blakemore, T. B. Marder and P. G. Steel, *J. Org. Chem.*, 2015, **80**, 5308–5314.

15 S. A. Sadler, H. Tajuddin, I. A. I. M Khalid, A. S. Batsanov, D. Albesa-Jove, M. S. Cheung, A. C. Maxwell, L. Shukla, B. Roberts, D. C. Blakemore, Z. Lin, T. B. Marder and P. G. Steel, *Org. Biomol. Chem.*, 2014, **12**, 7318–7327.

16 A. J. J. Lennox and G. C. Lloyd-Jones, *Chem. Soc. Rev.*, 2014, **43**, 412–443.

17 Z. Dong, G. C. Clososki, S. H. Wunderlich, A. Unsinn, J. Li and P. Knochel, *Chem.-Eur. J.*, 2009, **15**, 457–468.

18 T. dos Santos, H. P. Orenha, V. E. Murie, R. Vesseccchi and G. C. Clososki, *Org. Lett.*, 2021, **23**, 7396–7400.

19 M. Balkenhohl, B. Salgues, T. Hirai, K. Karaghiosoff and P. Knochel, *Org. Lett.*, 2018, **20**, 3114–3118.

20 V. Giannouli, N. Lougiakis, I. K. Kostakis, N. Pouli, P. Marakos, A.-L. Skaltsounis, S. Nam, R. Jove, D. Horne, R. Tenta, H. Pratsinis and D. Kletsas, *Bioorg. Med. Chem. Lett.*, 2016, **26**, 5229–5233.

21 A.-M. Fantel, V. Myrianthopoulos, A. Georgoulis, N. Lougiakis, I. Zantza, G. Lamprinidis, F. Augsburger, P. Marakos, C. E. Vorgias, C. Szabo, N. Pouli, A. Papapetropoulos and E. Mikros, *Mol.*, 2020, **25**, 3739.

22 D. Matsuda, Y. Kobashi, A. Mikami, M. Kawamura, F. Shiozawa, K. Kawabe, M. Hamada, K. Oda, S. Nishimoto, K. Kimura, M. Miyoshi, N. Takayama, H. Kakinuma and N. Ohtake, *Bioorg. Med. Chem. Lett.*, 2016, **26**, 3441–3446.

23 N. Lougiakis, P. Marakos, N. Pouli and J. Balzarini, *Chem. Pharm. Bull.*, 2008, **56**, 775–780.

24 A. Papastathopoulos, N. Lougiakis, I. K. Kostakis, P. Marakos, N. Pouli, H. Pratsinis and D. Kletsas, *Eur. J. Med. Chem.*, 2021, **218**, 113387.

25 C. Wang, Y. Pei, L. Wang, S. Li, C. Jiang, X. Tan, Y. Dong, Y. Xiang, Y. Ma and G. Liu, *J. Med. Chem.*, 2020, **63**, 6066–6089.

